Preparation of carbon microcoils/nanocoils and ceramic microcoils, and their properties

○**S. Motojima (Gifu University)**, H. Iwanaga and T. Hashishin (Nagasaki University), T. Kojima and T. Tsuda (Nagoya Institute of Technology)

Introduction

Ceramic springs/coils made by silicon nitride with only several mm~several ten mm coil diameters are now commercially available. The ceramic spring/coils are very useful because they can be used at high temperatures up to 1000℃ and in corrosive atmospheres without reducing their strength and elasticity. However, the ceramic spring/coils are not widely used because of their high cost due to their complex preparation procedures.

We first prepared the silicon nitride (Si_3N_4) microcoils with the coil diameter of 20-30 μm and coiling numbers of 10-15 turns by the catalytic CVD process. Furthermore, we prepared the carbon microcoils with the coil diameter of 5-10 μm and coil length of 1-5 mm by the catalytic pyrolysis of acetylene, and examined the preparation conditions, morphology, growth mechanism and some properties. The microcoils made by silicon nitride or carbon (carbon microcoils) have a 3D-helical/spiral structure similar to a DNA (deoxynucleic acid) or proteins. Accordingly, these microcoils have potential applications as micromechanical devices, electromagnetic wave absorbers, microsensors, microdevices, microactuators, gas absorbers, chiral catalysts, etc.

In this review, we introduce the new measurement procedures of the microcoils made of silicon nitride and carbon obtained by the catalytic CVD process, and then describe the mechanical and electrical properties of the microcoils.

1) New measurement procedures of the elastic properties of ceramic microcoils: Carbon microcoils easily extend by several times and more their original coil length under a small applied load of 3-30mgf. Accordingly, a commercial tensile strength instrument can not be used. We devised a new measurement apparatus for obtaining the elastic properties of the microcoils, and such a measurement cell is shown Fig. 1. The two ends of a microcoil is adhered to a thin straight fiber such as a carbon fiber. One end of the thin fiber is adhered to a slide glass which is placed on an inclinable optical microscope, and the other is adhered to the cover glass. The slide glass is gradually inclined while focusing on the microcoils. The microcoil extends with an increasing inclination angle and the tension ratio linearly increases with the increasing inclination angle. The applied load (W) to the microcoils can be estimated by eq.1,

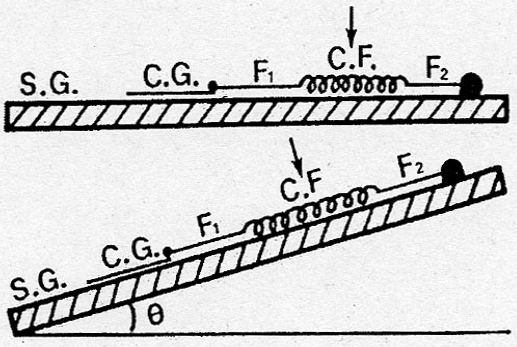

Fig. 1. Stretching process of microcoils using the inclinable optical microscope.
S.G.: slide glass, C.G.: cover glass, F_1 and F_2: straight carbon fiber. Arrow indicates the focusing and observing point.

$$W = W_0 (\sin\theta - \mu\cos\theta) \quad (1)$$

where W_0 is the weight of the cover glass, μ is the static friction coefficient, and θ is the inclination angle. The static friction coefficient (μ) was about 0.35 when alumina powder of 60-80 μm diameter was inserted between the cover glass and slide glass, The shear modulus (G) and shearing strength (τ_{max}) can be estimated by eqs. 2 and 3,

$$G = (64nr^3/d^4)(W/\rho) \quad (2)$$

$$\tau_{max} = 16rW_{max}/\pi d^3 \quad (3)$$

where n is the pitch number, r is the coil radius and d is the fiber diameter. Furthermore, W_{max} is the applied load at which microcoils is ruptured.

2) Steel spring: Fig. 2 shows the smallest commercially available steel spring. The coil diameter is about 0.4 mm. Fig. 3 shows the extended steel coil. The steel coil could not recover to its original spring length after it was extended up to 1.3 times its original coil length. The stress-strain (s-s) curve of the metal spring

2002 INTERNATIONAL SYMPOSIUM ON MICROMECHATRONICS AND HUMAN SCIENCE
0-7803-7611-0/02/$17.00

is shown in Fig. 4. The shear modulus (G)

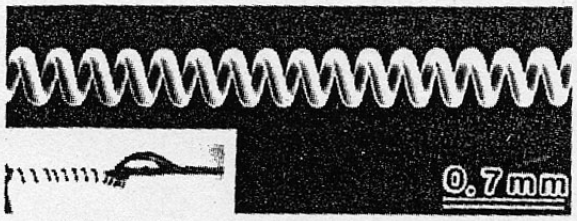

Fig. 2. Steel spring.
Under left-inserted figure shows the Si_3N_4 microcoils.

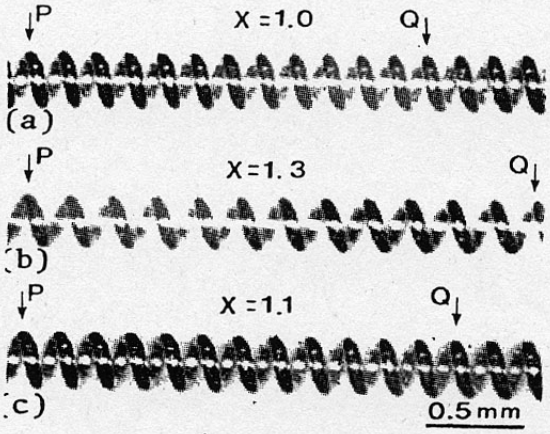

Fig. 3. Extension characteristics of steel spring.
(a) Original state, (b) extended state, (c) released state after the extension in (b). Inclination angle (θ)(deg): (a) 0, (b) 60, (c) 0, X: extension ratio.

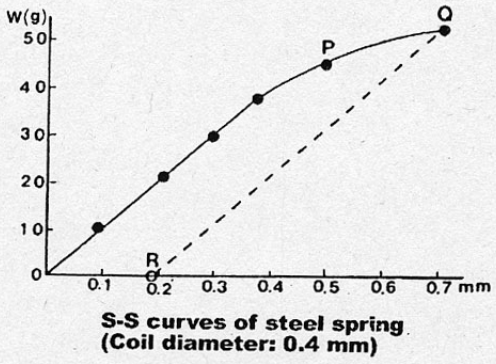

Fig. 4. Stress-strain (s-s) curves of the steel spring.

within the elastic limit region was estimated to be $8.8x10^3$ kg/mm^2. This value is comparable to that of reported values. That is, this new process is a reliable measurement process for obtaining the mechanical properties of microspring/microcoils.

3) Si_3N_4 microcoils: The Si_3N_4 microcoils can be obtained by the catalytic CVD process using a Si_2Cl_6+H_2 gas mixture as the source gas at 1200 ℃. Fig. 5 shows the representative Si_3N_4 microcoils. The Si_3N_4 microcoils have a fiber diameter of 2-3 μ m, 5

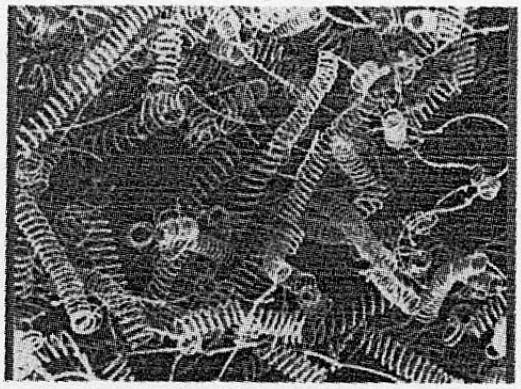

Fig. 5. Representative Si_3N_4 microcoils.

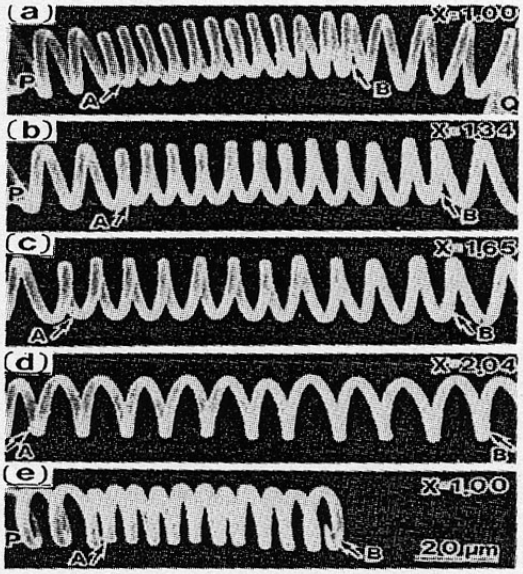

Fig. 6. Extension characteristics of the Si_3N_4 microcoils (1).X: extension ratio. (a) original state, (b-d) extended state, (e) ruptured coils after extended above X=2.04 (b).

coil diameter of 20-30 μ m, coil pitch of 2- μ m, and coil number of 10-15 turns. Fig. 6 shows the extension characteristics of the Si_3N_4 microcoils. The microcoils were ruptured after their extension of more than 2 times their original coil length. The coil length (separation of A-B in Fig. 6(a) and 6(d)) is the same indicating that these microcoils returned to their original coil length after they had ruptured. Fig. 7 shows the extension characteristics of the Si_3N_4 microcoils with increasing inclination angle. In this case, the Si_3N_4 microcoils extended to more than 3 times. The s-s curve of the Si_3N_4 microcoils is shown in Fig. 8. The shear modulus (G) was 13-16X10^3 kg/mm^2.

4) Carbon microcoils: The carbon microcoils with a 3D-helical/spiral structure can be obtained by the catalytic pyrolysis of acetylene at 750-800℃. The carbon coils

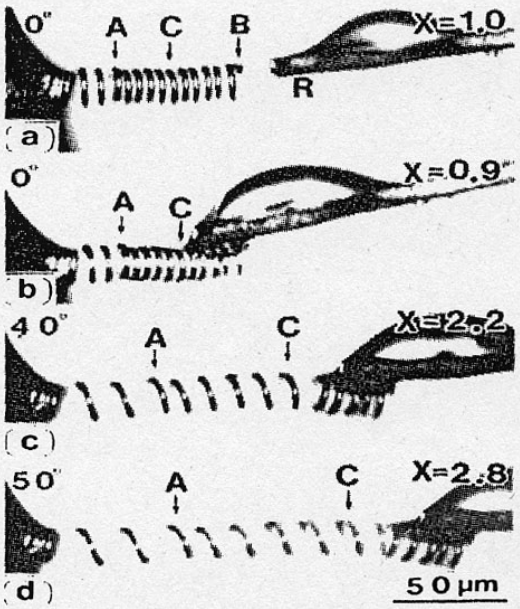

Fig. 7. Extension characteristics of the Si_3N_4 microcoils (2) as a function of inclination angle.

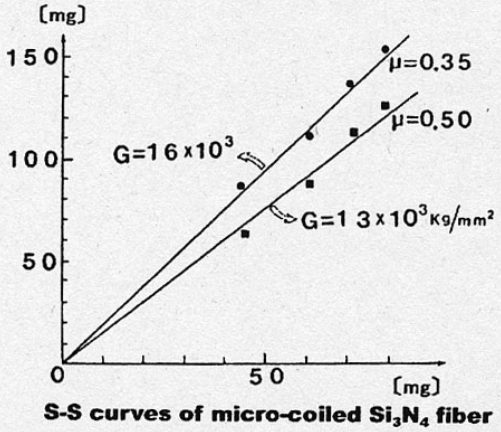

Fig. 8. Stress-strain (s-s) curve of the Si_3N_4 microcoils. G: shear modulus, μ : friction coefficient.

grow on a substrate painted with the metal catalyst fine particles, and the coil layers formed on the substrate surface reached 5-10 mm thick after 1–2 hr reaction times as shown in Fig. 9. The carbon coils, on the tip of which a metal catalyst grain is present, grows perpendicular to the substrate surface pointing the tip to the source gas inlet as shown in Fig. 10. Fig. 11 shows the enlarged view of the representative regular circular carbon coils with a circular or elliptical fiber cross-section. The carbon coils are generally double coils like DNA(deoxynucleic acid). The number of carbon coils of the right-clockwise and left-clockwise type was generally the same, while the coiling direction within a coil is the same direction. The carbon coils are generally densely coiled with a constant coil

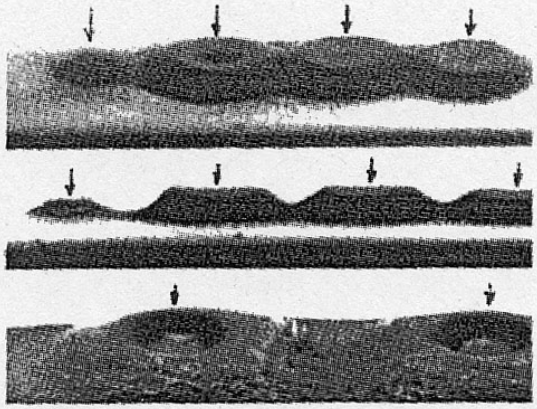

Fig. 9. Carbon microcoil layers grown on a graphite substrate. Arrow indicates the source gas inlet.

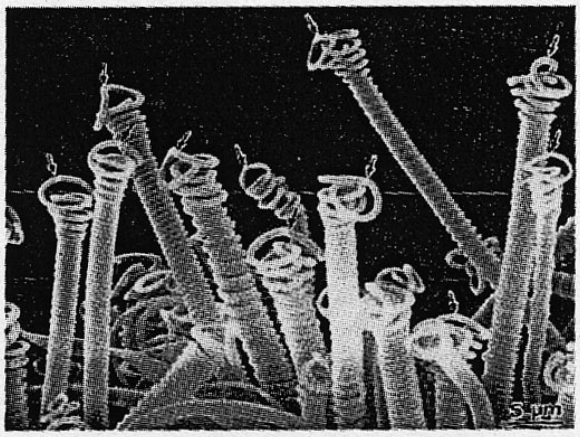

Fig. 10. Tip part of the carbon microcoils. Arrow indicated the catalyst grain.

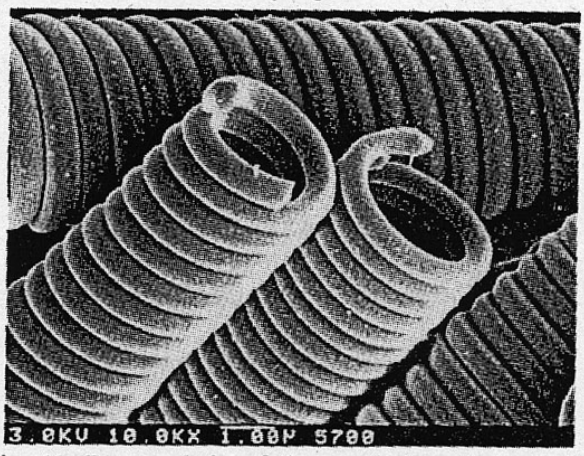

Fig. 11. Ruptured tip of the regularly-coiled circular carbon microcoils with a circular or elliptical fiber cross-section.

diameter and coil pitch and without a coil gap within a coil. Figs. 12 and 13 shows the regular flat carbon coils with the flat or ribbon-like form in fiber cross-section. The carbon coils obtained at a 30 min reaction time or more are generally these regular flat coils. By controlling the reaction conditions, the carbon coils with large coil diameters of 20-50 μm can be obtained (Fig. 14). The single coils such as shown in Fig. 15 are also sometimes obtained. The carbon nanocoils

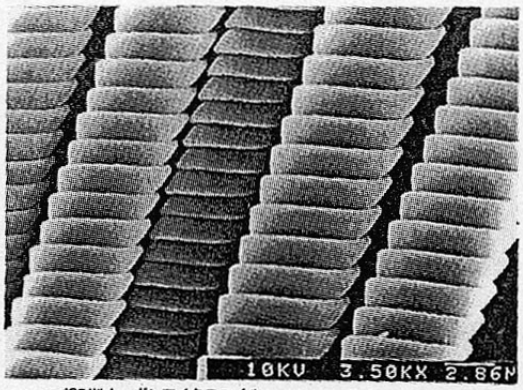

規則性カーボンマイクロコイル
（多くのコイルは、断面が扁平なカーボンファイバーから成され、一定のコイル径で非常に規則的に巻いており、コイル長さは5-10 mmに達する）

Fig. 12. Regularly-coiled flat carbon microcoils with a flat or ribbon-like fiber cross-section.

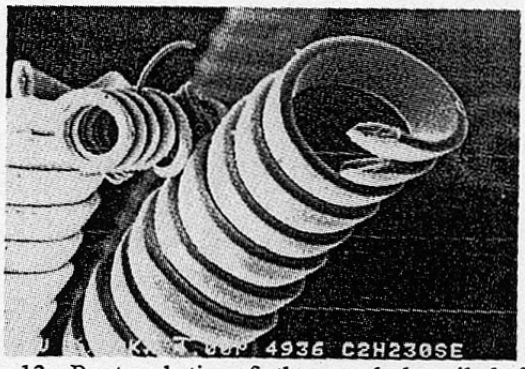

Fig. 13. Ruptured tip of the regularly-coiled flat carbon microcoils.

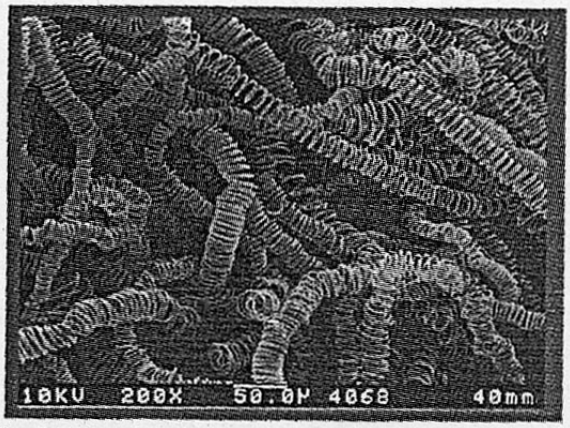

Fig. 14. Carbon microcoils with a large coil diameter.

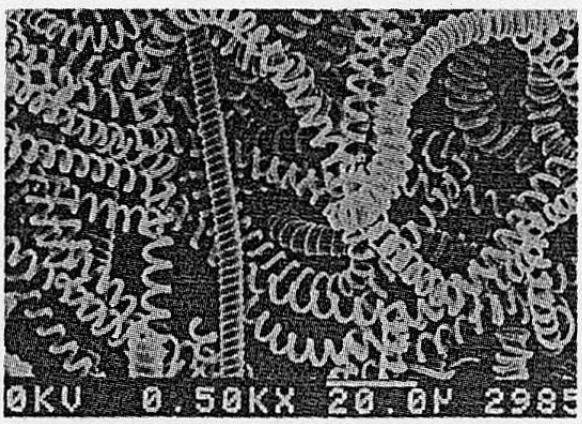

Fig. 15. Single carbon microcoils.

with a coil diameter below submicrons are generally a single coil. The carbon microcoils are amorphous and have excellent elasticity. Fig. 16 shows the extension patterns of the regular carbon coils without a coil gap. The regular carbon coils extend stepwise as shown in Fig. 17, because thin carbon layers are deposited in the coil gap and the two adjacent coils weakly adhere to each other. After the coils were once fully extended, generally above 1.5 times, the coils can be smooth and continuously extended. The carbon microcoils with a circular fiber cross section (Fig. 11) or large coil diameters (Figs. 14) can be extended up to 10 times their original coil length, while the flat carbon coils with a flat or ribbon-like fiber cross section (Figs. 12 and 13) can only be extended by 1.5-3 times their original coil length. Fig. 18 shows the extension patterns of the coil layers by tweezers. The coil layers can be extended up to 25mm as shown in Fig. 18 (A → C).

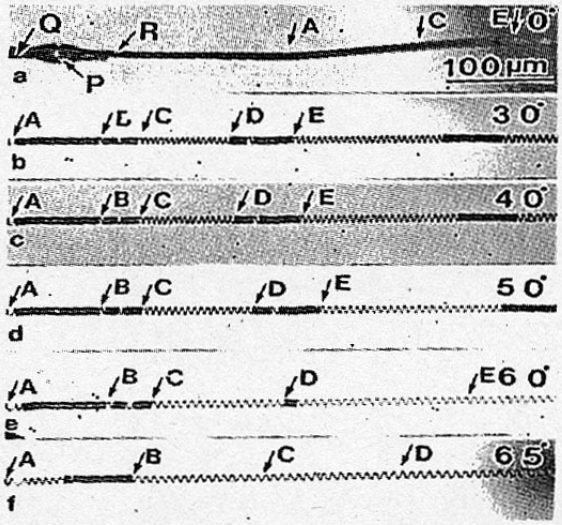

Fig. 16. Stepwise extension increase in regular flat carbon microcoils with increasing inclination angle.

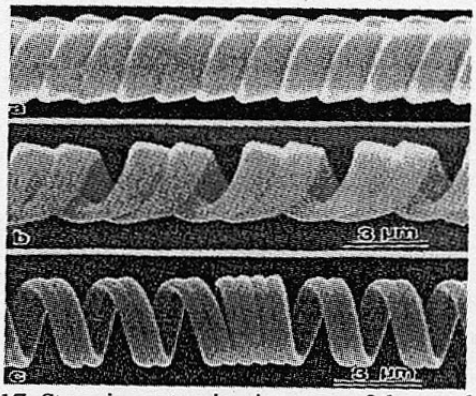

Fig. 17. Stepwise extension increase of the regular flat carbon microcoils.

Furthermore, the extended coil layers quickly contracted to the original layer level after

releasing the pulling load as shown in Fig. 18(C→D). Fig. 19 shows an enlarged view of the extended carbon microcoils. It can be seen that the carbon coils extend to a nearly straight form while maintaining the double coiling structure.

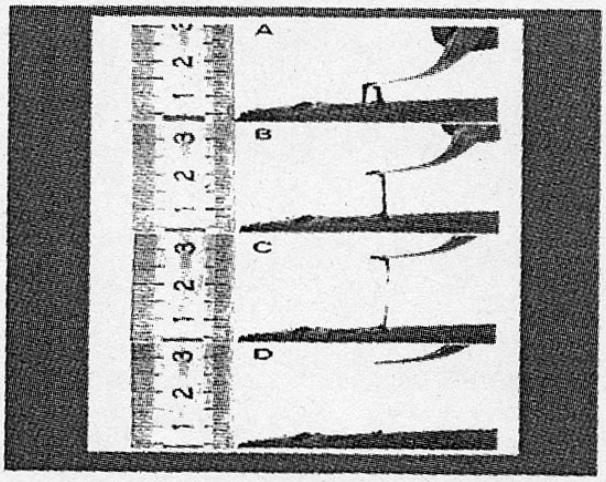

Fig. 18. Stretching of the carbon coil layers by tweezers. (D) indicates the recovered state after releasing the pulling force in (C).

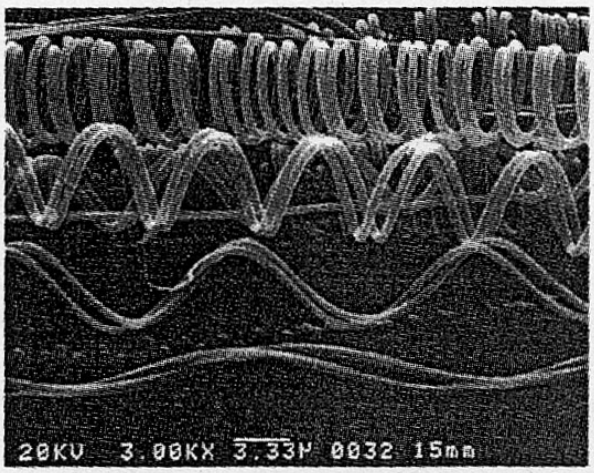

Fig. 19. Various extension states of the carbon microcoils.

The current-voltage (i-v) characteristics of a piece of regular carbon coils were measured using a measurement cell as shown in Fig. 20. The obtained i-v characteristics are shown in Fig. 21, in which the as-grown carbon coils and the coils once stretched 1.5 times and contracted to the original coil length for avoiding the effect of thin carbon layers deposited in the coil gap. It can be seen that the current superlinearly increases up to about 570 μA with the increasing applied voltage and that at a 40 V applied voltage, the current abruptly decreased due to burn out of the coils. On the other hand, the

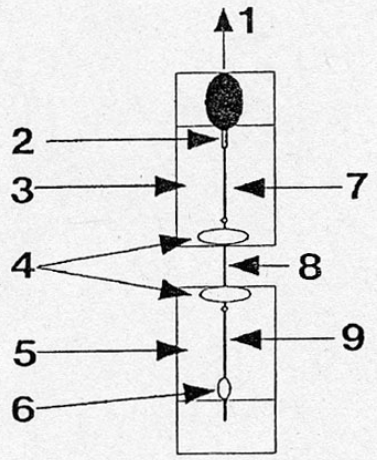

Fig. 20. Measurement cell used for the extension characteristics and electrical conduction of the carbon microcoils. (1) Manipulator, (2) thin wire, (3 and 5) electrode, (4) Ag conductive paste, (6) adhesive agent, (7 and 9) thick fiber, (8) a piece of carbon microcoil.

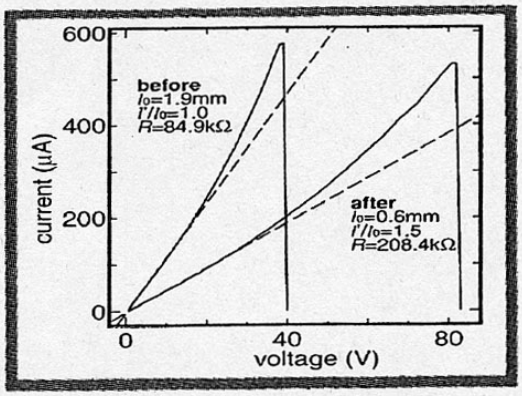

Fig. 21. Current-voltage (i-v) characteristics of a carbon microcoil piece. (Before): as-grown carbon microcoils, (after): carbon microcoils which was once extended by 1.5 times and then recovered to original state.

carbon coils once expanded to 1.5 times burn out at 80V. The resistivity of the as-grown and expanded carbon coils were 84.9 k Ω and 208.4 k Ω , respectively. These results suggest that the thin carbon layers deposited in the coil gap act as an effective conduction path. Fig. 22 shows the temperature dependence of the electrical resisitivity of the carbon coils. The resistivity decreased with increasing temperature thus showing their semiconductive characteristics. Fig. 23 shows the effect of the tension ratio on the electrical resistivity of three pieces of carbon microcoils. The resitivity stepwise increases with the increasing expansion ratio. This stepwise increase in the resistivity corresponds to that of the

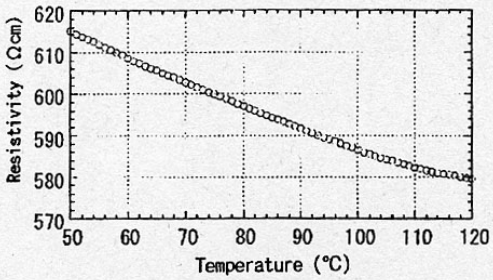

Fig. 22. Electrical resistivity of a piece of carbon microcoil as a function of the temperature.

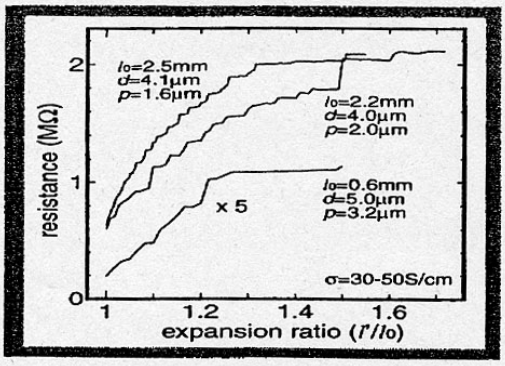

Fig. 23. Relationship between electrical resistivity of the carbon microcoils and extension ratio. (l`) Coil length after extension, (l_o) original coil length.

stepwise stretch of the coils as shown in Fig. 16. The electrical conductivity is estimated to be 30-50 S cm^{-1}. Fig. 24 shows the effect of the tension ratio of the carbon coils, which was once expanded by 1.5 times, on the electrical resistivity ratio versus the resistivity without an extension. It can be seen that the resistivity of the carbon coils generally increases with the tension ratio probably caused by the inner stress generation due to the large extension. The carbon microcoils can be easily extended under very low loads of 10-50 mg. Figs. 25 and 26 show the measurement apparatus and cell for obtaining the s-s curve of a piece of coil. The carbon microcoils with a load was pulled up by a 3D-manipulator and the applied weight change was obtained as the weight decrease using a precise electron balance. Fig. 27 shows the s-s curve of the two flat carbon microcoils. The coils linearly extend with the increasing applied load. The extension ratio for coils A and B were 1.9 times and 2.5 times, respectively. The elastic modulus was estimated to be 4.4 GPa for coil A and 9.3 GPa for coil B. Fig. 28 shows the s-s curves of the circular carbon microcoils. It can be seen that the circular carbon microcoils extend under a very low applied

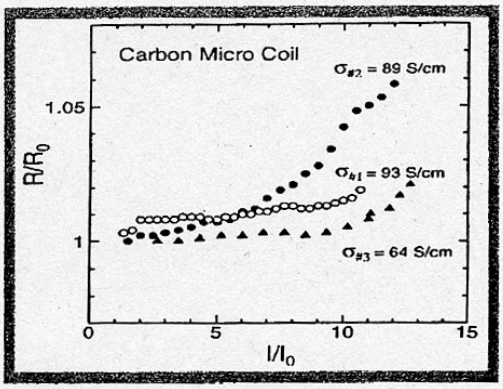

Fig. 24. Relationship between resistivity ratio of a piece of carbon microcoil and the expansion ratio. (R) electrical resistivity of the extended carbon microcoils, (R_o) original resistivity.

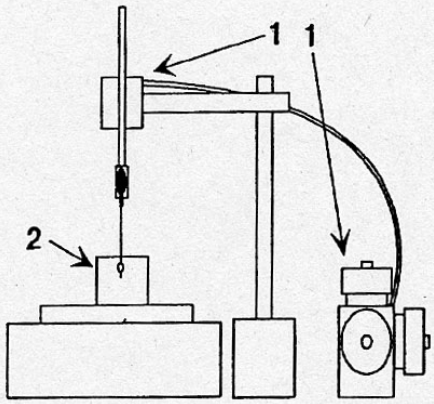

Fig. 25. Measurement apparatus of the mechanical properties (s-s curve) of the carbon microcoils. (1) 3D-manipulator, (2) weight.

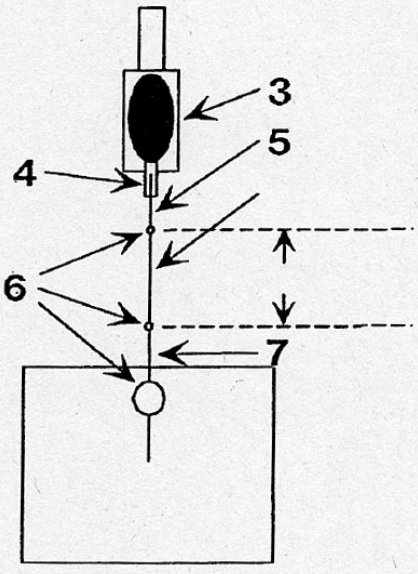

Fig. 26. Measurement cell.
(2) Compound, (4) wire, (5 and 7) thick fiber, (6) adhesive agent. Arrow indicates a piece of carbon microcoil and its length.

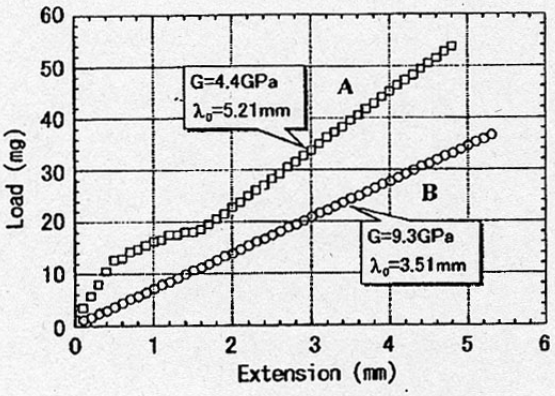

Fig. 27. S-s curves of different carbon microcoils.

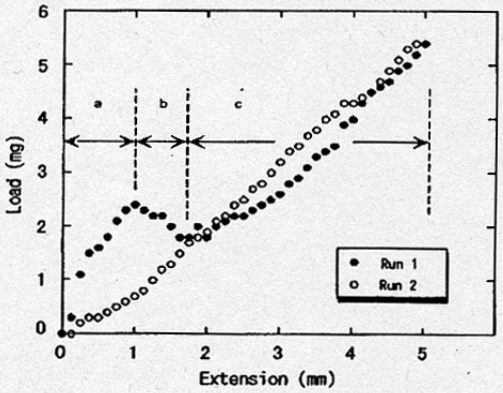

Fig. 28. S-s curves of carbon microcoils.
Run 1 shows the initial stretching and run 2 shows the second stretching of the once stretched coils in Run 1.

load of 1/10 that of the flat coils as shown in Fig. 27. The electrical resistivity fluctuates with time as shown in Fig. 29, while the fluctuation can be decreased by the parallel insertion of a 10 μF capacitor as shown in Fig. 29(b) and no fluctuation was observed for the carbon film capacitor (c). These results suggest that the current conduction of the carbon microcoils is sensitively affected by white noises such as electromagnetic waves.

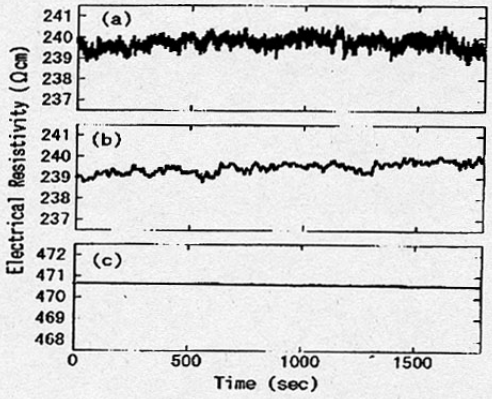

Fig. 29. Time fluctuation of the electrical resistivity.
(a and b) carbon coils, (c) carbon layer capacitor.
(a and c) by usual measurement, (b) by parallel insertion of 10 μF capacitor.

An alternative current was applied to the carbon microcoils, and the extension and contraction characteristics were measured using the apparatus shown in Fig. 30. One terminal of the carbon microcoils was fixed to one electrode and other terminal was immersed in distilled water in which the other electrode was attached as shown in Fig. 31. The alternative current was applied between two electrodes, and the motion of the coils was observed by a CCD camera. It was observed that the carbon coils expands and contracts in the same cycle with the frequency of the applied AC as shown in Figs. 32 and 33. The reason for these interesting phenomena is not yet known.

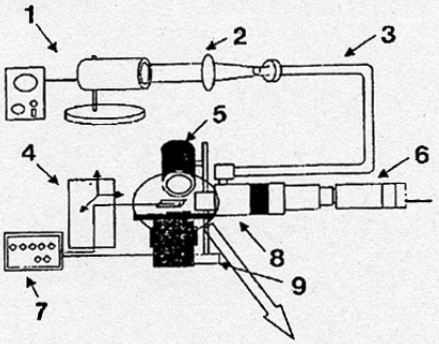

Fig. 30. Measurement apparatus of actuation property.
(1 and 5) light source, (2) lens, (3) optical fiber, (6) CCD camera, (7) function generator, (8) high magnification zoom lens, (9) XYZ piezo stage,

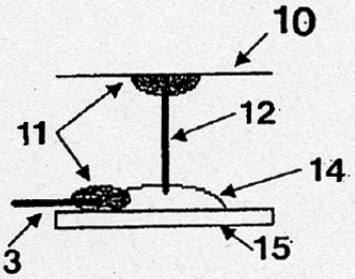

Fig. 31. Measurement cell.
(10) Cover glass, (11) Ag conductive paste, (12) carbon microcoils, (13) electrode, (14) distilled water, (15) slide glass.

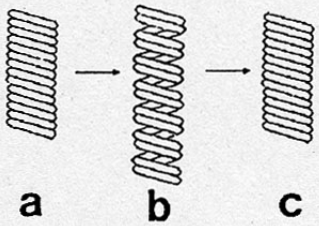

Fig. 32. Extension and contraction action pattern.
(a and b) without application of AC, (b) with application of AC.

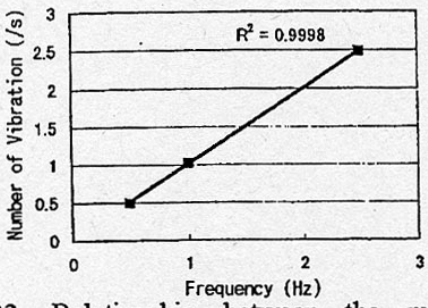

Fig. 33. Relationship between the number of vibrations and frequency of applied AC.

Corresponding Author:
S. Motojima: (Tel) 058-293-2621, (Fax) 058-293-5012,
(e-mail) motojima@apchem.gifu-u.ac.jp

References

1) Morphology of coiled whiskers of amorphous Si3N4 and their mechanical properties, H. Iwanaga, et al., J. Mater. Sci. Eng., 9(1990)731.
2) Impurity-acitvated chemical vapor growth of micro-coiled carbon fibers, S. Motojima, et al., J. Chem. Vapor Deposition, 3(1994)87-
3) Elecrical properties of carbon microcoils, K. Kaneto, et al., Synthetic Met., 103(1999)2578.
4) Vapor phase preparation of cosmomimetic-carbon microcoils and their properties, X. Chen, et al., Trans. Mater. Res. Soc. Jpn., 25(2000)565.
5) Vapor phase preparation of super-elastic carbon microcoils, X. Chen, et al., J. Cryst. Growth, 237-239(2002)1931.